Tetracycline Treatment Retards the Onset and Slows the Progression of Diabetes in Human Amylin/Islet Amyloid Polypeptide Transgenic Mice

Jacqueline F. Aitken,[1,2] Kerry M. Loomes,[1,2] David W. Scott,[1,3] Shivanand Reddy,[1] Anthony R.J. Phillips,[1,2,4] Gordana Prijic,[1] Chathurini Fernando,[1] Shaoping Zhang,[1,2] Ric Broadhurst,[5] Phil L'Huillier,[5] and Garth J.S. Cooper[1,2,3,6]

OBJECTIVE—Aggregation of human amylin/islet amyloid polypeptide (hA/hIAPP) into small soluble β-sheet–containing oligomers is linked to islet β-cell degeneration and the pathogenesis of type 2 diabetes. Here, we used tetracycline, which modifies hA/hIAPP oligomerization, to probe mechanisms whereby hA/hIAPP causes diabetes in hemizygous hA/hIAPP-transgenic mice.

RESEARCH DESIGN AND METHODS—We chronically treated hemizygous hA/hIAPP transgenic mice with oral tetracycline to determine its effects on rates of diabetes initiation, progression, and survival.

RESULTS—Homozygous mice developed severe spontaneous diabetes due to islet β-cell loss. Hemizygous transgenic animals also developed spontaneous diabetes, although severity was less and progression rates slower. Pathogenesis was characterized by initial islet β-cell dysfunction followed by progressive β-cell loss. Islet amyloid was absent from hemizygous animals with early-onset diabetes and correlated positively with longevity. Some long-lived nondiabetic hemizygous animals also had large islet-amyloid areas, showing that amyloid itself was not intrinsically cytotoxic. Administration of tetracycline dose-dependently ameliorated hyperglycemia and polydipsia, delayed rates of diabetes initiation and progression, and increased longevity compared with water-treated controls.

CONCLUSIONS—This is the first report to show that treating hA/hIAPP transgenic mice with a modifier of hA/hIAPP misfolding can ameliorate their diabetic phenotype. Fibrillar amyloid was neither necessary nor sufficient to cause diabetes and indeed was positively correlated with longevity therein, whereas early- to mid-stage diabetes was associated with islet β-cell dysfunction followed by β-cell loss. Interventions capable of suppressing misfolding in soluble hA/hIAPP oligomers rather than mature fibrils may have potential for treating or preventing type 2 diabetes. *Diabetes* **59:161–171, 2010**

Type 2 diabetes is a chronic hyperglycemic disorder caused by defective action and/or secretion of insulin, which manifests with complications that ultimately cause most of its morbidity and mortality. It is also an amyloidosis, since it is accompanied by amyloid deposits in regions of tissue degeneration and β-cell loss in the islets of Langerhans (1,2). These deposits (3) comprise mainly fibrillar aggregates of a 37–amino acid monomer, human amylin (hA)/islet amyloid polypeptide (hIAPP) (4,5) (the term hA/hIAPP has been used to reflect the two names commonly used for this peptide hormone), which is secreted from the β-cells.

Islet amyloid is associated with substantial reductions in relative β-cell mass in type 2 diabetes (on average ~60%), probably due to increased apoptosis compared with obese and lean nondiabetic humans (2). An inability to adaptively compensate β-cell mass in type 2 diabetes has been postulated to lead to or cause an absolute insulin deficiency over time with a resulting requirement for insulin replacement therapy in affected subjects (1).

Several lines of evidence now provide compelling support for the idea that processes associated with hA/hIAPP aggregation contribute to β-cell degeneration. First, in vitro studies with synthetic hA/hIAPP preparations show that fibrillar structures are generated spontaneously through self-association of monomers into protofibrils and higher-order fibrils (6). Cytotoxic hA/hIAPP preparations contain few preformed fibrils but undergo time-dependent aggregation into soluble β-conformers (7). β-Cell toxicity evoked by aggregating extracellular hA/hIAPP occurs through an apoptotic mechanism (8,9) mediated via a pathway comprising initial activation of a membrane-bound Fas/FasL/FADD/caspase-8 complex (10) followed by a three-pronged downstream cascade comprising c-Jun NH_2-terminal protein kinase 1/cJun (11), activating transcription factor 2/p38 mitogen-activated protein kinase (12), and p53/p21$^{WAF1/CIP1}$ (9) that leads ultimately to activation of caspase-3 (13). In addition, parallel amylin-mediated activation of endoplasmic reticulum stress–related pathways may contribute to islet β-cell degeneration (14).

Second, associations between hA/hIAPP aggregation and decreased β-cell mass have been reported from in vivo studies (15–19) in several murine transgenic models of hA/hIAPP-mediated diabetes. By contrast, mA/mIAPP molecules do not aggregate, so diabetic phenotypes in hA/hIAPP transgenic mice develop in a background devoid of amyloid formed by mA/mIAPP. Obese hA/hIAPP trans-

genic mice have been reported to replicate pathological findings of human type 2 diabetes, showing nonketotic hyperglycemia, amyloid deposition, and decreased β-cell mass, possibly via increased apoptosis (18).

These data support a hypothesis that hA/hIAPP aggregation could mediate β-cell failure in type 2 diabetes. However, the significance of mature amyloid fibrils in the pathogenesis of this process is still uncertain, as is whether hA/hIAPP-mediated cytotoxicity can be abrogated by in vivo treatment with amylin-binding compounds. Peptide-based analogs that bind amyloid-forming structural motifs within hA/hIAPP have reportedly inhibited aggregation of synthetic hormone in vitro, with concomitant suppression of cytotoxicity in cultured β-cells (20), but in vivo efficacy of this therapeutic approach has yet to be reported.

Here, we have generated lines of hA/hIAPP transgenic mice that spontaneously develop diabetes. Phenotypes vary from early-onset diabetes without microscopically detectable amylin aggregates to late-onset diabetes with microscopic amyloid deposits. Diabetes pathogenesis and progression in hemizygous animals occurs primarily through islet β-cell dysfunction with subsequent β-cell loss. Both onset and progression were significantly inhibited by chronic treatment with tetracycline, an antibiotic that interacts with aggregates of proteins implicated in amyloid-related diseases (21–23).

RESEARCH DESIGN AND METHODS

Ethics approval. Experimental protocols were approved by the University of Auckland Animal Ethics Committee and performed in accordance with the New Zealand Animal Welfare Act (1999).

Materials. Chemicals and kits were from Roche Applied Biosciences, Invitrogen, Life Technologies/BRL, or Sigma and were of analytical grade or better, unless stated otherwise.

Generation of hA/hIAPP transgenic mice. The hA/hIAPP transgene (supplemental Fig. S1A [available at http://diabetes.diabetesjournals.org/cgi/content/full/db09-0548/DC1]) was constructed from PCR-derived fragments using the following primer pairs: RIP5 (GAAAGACTCGAGGATCCCCCAACCAC) and RIP3 (CAGGGCCATGGTGGAACAATGACC), hAMY5 (GAAGCCATGGGCATCCTGAAGCTGCAAGTA) and hAMY3 (GTCATGTGCACCTAAAGGGGCAAGTAATTCA), hALB5 (GTGTGTTTCATCGATATGCACGTAAGAAA) and hALB3 (CAACCTCAAGCTTGTCTGGGCAAGGG), hGAPDH5 (GGAGTAAGCTTCCTGGACCACCAGCCCC), and hGAPDH3 (GTGCGAGTCT-AGACTTCCTCCACCTGTCA). It was introduced into the genome by pronuclear injection (24).

Northern analysis. RNA was extracted from liquid nitrogen snap-frozen tissues using QIAGEN RNeasy Midi Kits according with the rotor-stator tissue disruption (Ultra-Turrax T8; IKA-Werke, Germany). Total RNA (20 μg) was denatured and transferred to nylon membranes with $20\times$ SSC (25) and hybridized to ^{32}P-labeled probes (26) at 65°C overnight. Intensities of mRNA bands corresponding to hA/hIAPP and mA/mIAPP were not directly compared as experimental conditions differed (supplemental Fig. S1A and B).

Animal studies. Mice were fed ad libitum with Diet 86 (Tegel NRM, Auckland, Zealand), a dry-pelleted natural-ingredient diet with 3% fat. Blood glucose levels were determined in tail vein blood (Advantage II; Roche) and diabetes defined when concentrations were >11 mmol/l on two consecutive weekly readings. For survival studies, we applied an agreed euthanasia surrogate end point for death, consistent with current ethical practice. Euthanasia was performed in the following circumstances: after 20% loss of maximum body weight, if significant lethargy developed, following loss of exploratory behavior with increasing relative immobility, failure to groom, or any other signs of overt distress. Infection or malignancy were also accepted as indications for euthanasia.

Intraperitoneal insulin and glucose tolerance tests. Mice undergoing intraperitoneal insulin tolerance tests (ITTs) were typically fasted for 6 h. Thereafter, actrapid (0.5 mIU/g body wt; Novo Nordisk) was injected intraperitoneally in conscious animals (29 G needle). Glucose levels were measured before injection and at indicated times postinjection. For intraperitoneal glucose tolerance tests (GTTs), mice were overnight fasted

(16–18 h) with free access to water. Glucose was administered (1 mg glucose/g body wt) followed by tail blood sampling.

Blood and tissue extraction for hormone measurements. Cardiac puncture blood (EDTA) was separated (3,000g, 4°C, 15 min). Pancreata were excised and snap frozen (liquid nitrogen) and peptides extracted (homogenization, acid/ethanol) (27).

Hormone measurements. Murine insulin was determined in plasma, serum, or pancreatic extracts by Ultrasensitive Mouse Insulin enzyme-linked immunosorbent assay (ELISA) (Mercodia, Uppsala, Sweden) or rat/mouse insulin ELISA (Linco). Pancreatic extracts were diluted (1:500 and 1:5,000) in PBS (pH 7.4). Plasma hA/hIAPP was determined by ELISA (Linco) in plasma and pancreatic extracts; mA/mIAPP was determined using our in-house radioimmunoassay.

Pancreatic histochemistry and quantitative islet histomorphometry. Pancreatic tissue was paraffin embedded, serially sectioned (5 μm), and stained with hematoxylin and eosin. On adjacent sections, Congo red (1%; 15–20 min, then saturated lithium carbonate, 30 s) and hematoxylin staining were used to measure frequency and extent of islet amyloid (polarization microscopy). Islet morphology and amyloid content were analyzed by a single-blinded histologist who scored nine or more islets/animal. Pancreata were sectioned at sufficient levels (≥200 μm apart) to ensure analysis of ≥9 (but generally ~20–30) distinct islets/animal.

Immunohistochemistry. Representative sections were serially incubated with guinea pig anti-insulin serum, donkey anti-guinea pig IgG–fluorescein isothiocyanate, rabbit anti-glucagon, and donkey anti-rabbit IgG–Texas Red then counterstained with Congo red and reimaged to quantitate islet amyloid, morphology, and insulin and glucagon cells. Alternatively, sections were incubated with combined rabbit anti-glucagon and anti-somatostatin and imaged by indirect avidin-biotin-peroxidase.

Chronic oral administration of tetracycline. Tetracycline was administered orally via the drinking water in light-proof bottles either from the time of weaning (21 days of age) or from diabetes onset in different studies, at final concentrations (0.03 mg/ml or 0.5 mg/ml in water, 18 mol · lΩ^{-1} · cm^{-1}, milliQ; Millipore) and fresh solutions constituted weekly. Polydipsia was defined as fluid intake exceeding twice the average daily intake of the average nondiabetic adult mouse. Controls comprising hemizygous male mice and nontransgenic littermates received milliQ water alone.

Statistical analysis. Data were analyzed using GraphPad Prism 4 (GraphPad Software, San Diego, CA) and diabetes onset and survival using the Mantel-Haenszel log-rank test and the Gehan-Breslow-Wilcoxon test. Correlation analyses were performed using Pearson correlation with two-tailed hypotheses. Descriptive variables were contrasted by one-way ANOVA with Tukey-Kramer post hoc tests. Blood glucose and fluid intake values were contrasted using mixed models fitted by restricted maximum likelihood (JMP 5.1; SAS Institute). P values of <0.05 were considered significant.

RESULTS

Human amylin/hIAPP transgenic mice spontaneously developed diabetes. Transgenic animals were generated within a FVB/N background (supplmentary Fig. S1). One transgenic line, hereinafter designated as Line 13, had integrated transgene copy numbers of 36 ± 7 and 76 ± 2 for hemizygous and homozygous animals, respectively (data not shown).

Diabetes developed spontaneously and reproducibly in both homozygous and hemizygous Line 13 male and female mice, while nontransgenic littermates did not develop hyperglycemia (Fig. 1). All subsequent studies were performed in male animals (28,29). In homozygous mice, diabetes developed in 100% of animals ($n = 6$) by 41 days and all were dead by 91 days (Fig. 1A). By comparison, median values for time to diabetes onset and lifespan within the hemizygous group were longer (175 and 272 days, respectively) compared with homozygous animals (35 and 63 days, respectively). In addition, a second, independent line (designated Line 20) generated with the same construct and methods also developed spontaneous diabetes (Fig. 1A). Thus, the diabetic phenotype was not an artifact arising from insertional mutagenesis.

Intraperitoneal ITTs performed at 85 days showed that hemizygous mice developed spontaneous diabetes within a background of normal insulin sensitivity (Fig. 1B). Time
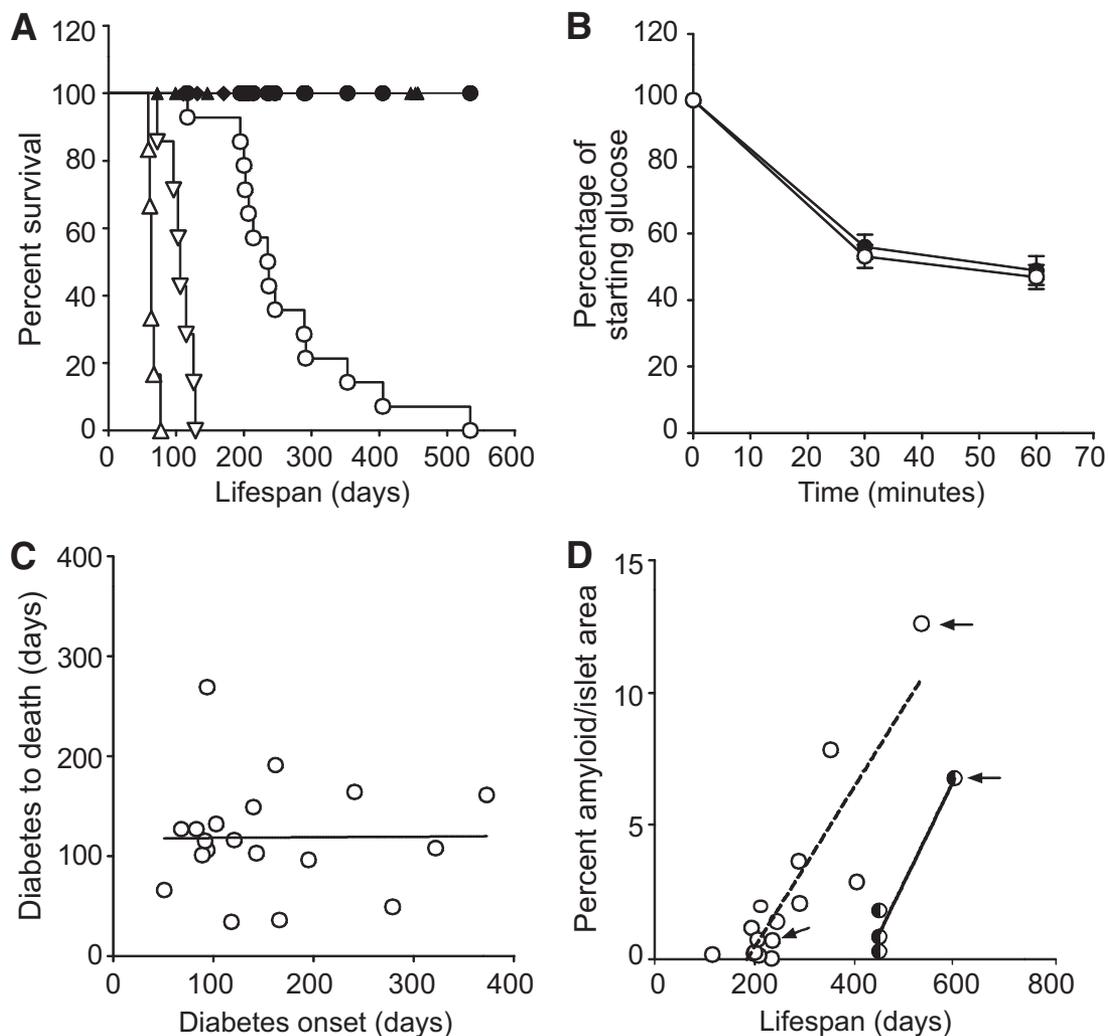
FIG. 1. Characterization of spontaneous diabetes in homozygous and hemizygous hA/hIAPP transgenic mice. *A*: Survival curves for two distinct lines of hA/hIAPP transgenic mice that were generated by separate injections of the same construct in the FVB/N background: homozygous line 13 ($\triangle$, $n = 6$); hemizygous line 13 ($\bigcirc$, $n = 14$); and hemizygous line 20 ($\triangledown$, $n = 7$). Closed symbols represent corresponding nontransgenic littermates. *B*: Intraperitoneal insulin tolerance tests in hemizygous line 13 mice ($\bigcirc$, $n = 11$) versus nontransgenic littermates ($\bullet$, $n = 6$) at 85 days of age. Animals were fasted overnight (17 h) then injected with Actrapid (0.75 mIU/g body wt). Data are means ± SE. *C*: Correlational analysis between time to diabetes onset and time of diabetes onset to death in hemizygous line 13 mice (P = NS, $n = 19$). *D*: Amyloid areas were positively correlated with lifespan in diabetic water-treated ($\bigcirc$, dashed line; $n = 14$, $R^2 = 0.78$, $P < 0.001$) and nondiabetic hemizygous animals (half-closed circles, $n = 4$, $R^2 = 0.95$, $P < 0.05$). Arrows indicate animals with representative islets shown in Fig. 2.

to diabetes onset was not correlated with the period between diabetes onset and death, showing that age did not influence the rate of progression of diabetes once it had begun (Fig. 1*C*).

Severity of diabetes progression was directly related to pancreatic expression of amyloidogenic human amylin. In homozygous mice, at an age where they were glucose intolerant (30 days; intraperitoneal GTTs not shown), plasma hA/hIAPP concentrations were 1.8-fold higher than in hemizygous animals and ~3.7-fold above nontransgenic control mA/mIAPP concentrations (Table 1). Normal plasma insulin was maintained in homozygous mice at 30 days despite a 72% reduction in pancreatic insulin content. Thus, at a time point similar to the median time to diabetes (35 days), substantial pancreatic insulin depletion had occurred in homozygous transgenic mice before a reduction in circulating insulin concentrations was detectable. Interestingly, and by contrast, pancreatic insulin concentrations in hemizygous animals were relatively unchanged at a time point (183 days) similar to the respective median onset time to diabetes (175 days).

These data indicated that an ~2- to 2.5-fold increase in expression of hA/hIAPP above endogenous and nonamyloidogenic mA/mIAPP in hemizygous animals was sufficient to evoke diabetes.

Amyloid deposition was dissociated from diabetes and positively correlated with lifespan. To investigate the relationship between amyloid deposition and diabetic phenotype, islet amyloid area was quantitated microscopically. Of the diabetic hemizygous animal cohort examined, there was a positive correlation between amyloid content and lifespan in animals that had survived >220 days (44% frequency, $P < 0.001$) (Fig. 1*D* and Fig. 2, *top two panels*). However, amyloid was rarely observed in terminally diabetic animals killed at lifespans <220 days (49% frequency). As expected, amyloid deposition was never observed in the islets of nontransgenic animals (Fig. 2, *middle panel*). Interestingly, some hemizygous animals remained nondiabetic (7% frequency) but showed the presence of islet amyloid (Fig. 1*D* and Fig. 2, *second to bottom panel*) with a similar relationship between amyloid content and lifespan as observed for diabetic hemizygous animals ($P < 0.05$). Amyloid

TABLE 1
Hormone concentrations in plasma and pancreatic tissue from fed wild-type (−/−) and hemizygous (+/−) and homozygous (+/+) hA/hIAPP transgenic mice at 30 days and 4 months of age

	Plasma (pmol/l)			Pancreas (pmol/mg)		
	Insulin	Human amylin	Murine amylin	Insulin	Human amylin	Murine amylin
30 days						
−/−	186 ± 39 (5)	ND (5)	19.4 ± 0.5*	798 ± 69 (5)	ND (4)	10.2 ± 1.4 (5)
+/−	157 ± 26 (15)	40 ± 4 (15)	—	799 ± 59 (15)	25 ± 2 (15)	—
+/+	177 ± 28 (5)	71 ± 15† (5)	—	221 ± 55‡ (5)	12 ± 5§ (5)	—
4 months						
−/−	269 ± 36 (12)	ND (12)	17.5 ± 1.3 (9)	1,261 ± 142 (8)	ND (9)	23.6 ± 1.6 (9)
+/−	238 ± 36 (19)	42 ± 5 (19)	—	1,028 ± 121(16)	28 ± 3 (16)	—

Data are means ± SE. The ELISA assay used to measure hA/hIAPP has a reported ≤1% cross-reactivity with human insulin, glucagon, glucagon-like peptide-1, pancreatic polypeptide, calcitonin, calcitonin gene–related peptide, and adrenomedullin and does not detectably cross-react with mA/mIAPP (39). The in-house radioimmunoassay used to measure mA/mIAPP had 7% cross-reactivity with hA/hIAPP and thus was used only in nontransgenic littermates. *Two pooled analyses representing a total of five animals. †$P < 0.05$, two-tailed t test. ‡$P < 0.001$ vs. both groups, one-way ANOVA with Tukey's post hoc test. §$P < 0.01$, two-tailed t test. —, not determined; ND, not detected.

was also absent from all terminally diabetic homozygous Line 13 mice analyzed (Fig. 2, *bottom panel*).

End-stage diabetes was characterized by selective loss of β-cells from the islets. Immunohistochemistry of pancreatic islet sections using antisera to stain both α- and δ-cells showed that almost all the islet cells in terminally diabetic homozygous and hemizygous mice were non–β-cells (Fig. 2). Glucagon staining also revealed a change in α-cell distribution from the physiological location at the islet periphery to a more dispersed distribution throughout diabetic islets, a substantive change in histomorphology (Fig. 2). Taken together, these findings show that end-stage diabetes in both homozygous and hemizygous animals was associated with islet β-cell loss and altered islet architecture. Consistent with these observations, plasma insulin and amylin concentrations in terminally killed homozygous and hemizygous animals were below the limits of detection (data not shown). We also performed studies for terminal deoxynucleotidyl transferase-mediated dUTP nick-end labeling and caspase-3 activation in islets from animals at different stages of diabetes, but rates were not significantly different between those from diabetic and control (nondiabetic) animals (results not shown). These findings are consistent with the observation that although apoptosis is widespread in biology, dying cells are seldom seen in situ because of their rapid clearance by phagocytosis (30). They do not, however, exclude the possibility that the sensitivity of the assays used may not have been sufficient to detect any differences in numbers of rare apoptotic cells.

Chronic oral administration of tetracycline (0.03 mg/ml drinking water) from weaning improved glycemic control and lifespan in hemizygous mice (study 1). We previously reported that tetracycline interacts with amylin fibrils based on evidence from thioflavin-T fluorescence and radioprecipitation assays (31). Here, we provide additional in vitro evidence for specific interactions between tetracycline and hA/hIAPP by circular dichroism spectroscopy (supplementary Fig. S2). In addition, to investigate whether tetracycline might modulate indexes of aggregation-evoked diabetes in vivo, hemizygous mice were randomly assigned to groups that were administered either water alone (control) or water containing 0.03 mg/ml tetracycline. Transgenic animals treated with tetracycline (0.03 mg/ml) developed diabetes with an apparently earlier median time to onset (85 days, $n = 17$) compared with those administered water only (121 days, $n = 20$), which is a difference that was

not significant by the Mantel-Haenszel log-rank test. As proportional hazards might not apply in this case, however, the data were reanalyzed using the Gehan-Breslow-Wilcoxon test, which does not rely on this assumption. The latter analysis did reveal a significant difference in median time to diabetes onset ($P < 0.05$). Following diabetes onset, progressive hyperglycemia resulted in the development of polydipsia at blood glucose concentrations of ~25 mmol/l (Fig. 3A and B). Since the upper limit of blood glucose measurement here was 33 mmol/l, the maximum reported values are lower-limit estimates of actual glucose concentrations in advanced diabetes.

Most importantly, in tetracycline-treated hemizygous animals, there was a significant delay in disease progression following onset of hyperglycemia, as measured by retardation in the rates of both blood glucose elevation (Fig. 3A, $P < 0.01$) and fluid intake (Fig. 3B, $P < 0.01$) compared with water-treated transgenic animals. Tetracycline had no effects on either blood glucose concentrations or fluid intake in nontransgenic littermates over the same time period. We did not quantitate blood tetracycline levels; however, assuming a similar bioavailability to oral doxycycline or minocycline administered to mice (32), we estimate that plasma tetracycline concentrations during the polydipsic phase could reach low micromolar levels. Survival analysis (Fig. 3C) showed that tetracycline-treated transgenic animals had a significantly increased median survival (34%, $P < 0.05$) for the period from diabetes onset to death (155 days, $n = 17$) compared with the water-treated control group (116 days, $n = 19$).

Examination of pancreata from terminally killed tetracycline-treated animals also showed a positive correlation between islet amyloid content and lifespan (Fig. 3D, $P < 0.001$, $n = 12$, $R^2 = 0.91$). This finding was similar to that observed for water-treated terminally diabetic hemizygous mice wherein the corresponding regression slope was not significantly different (Fig. 1D). Interestingly, of all the pancreata examined in this study the highest amyloid content occurred in a tetracycline-treated mouse, a finding consistent with the correspondingly increased lifespan observed in this group.

Tetracycline (0.5 mg/ml drinking water) improved glucose tolerance and delayed diabetes onset in hemizygous animals (study 2). To investigate whether the observed antidiabetes effects of tetracycline might be attributable to potential indirect insulin-sensitizing effects, parallel GTTs and ITTs were performed in independent
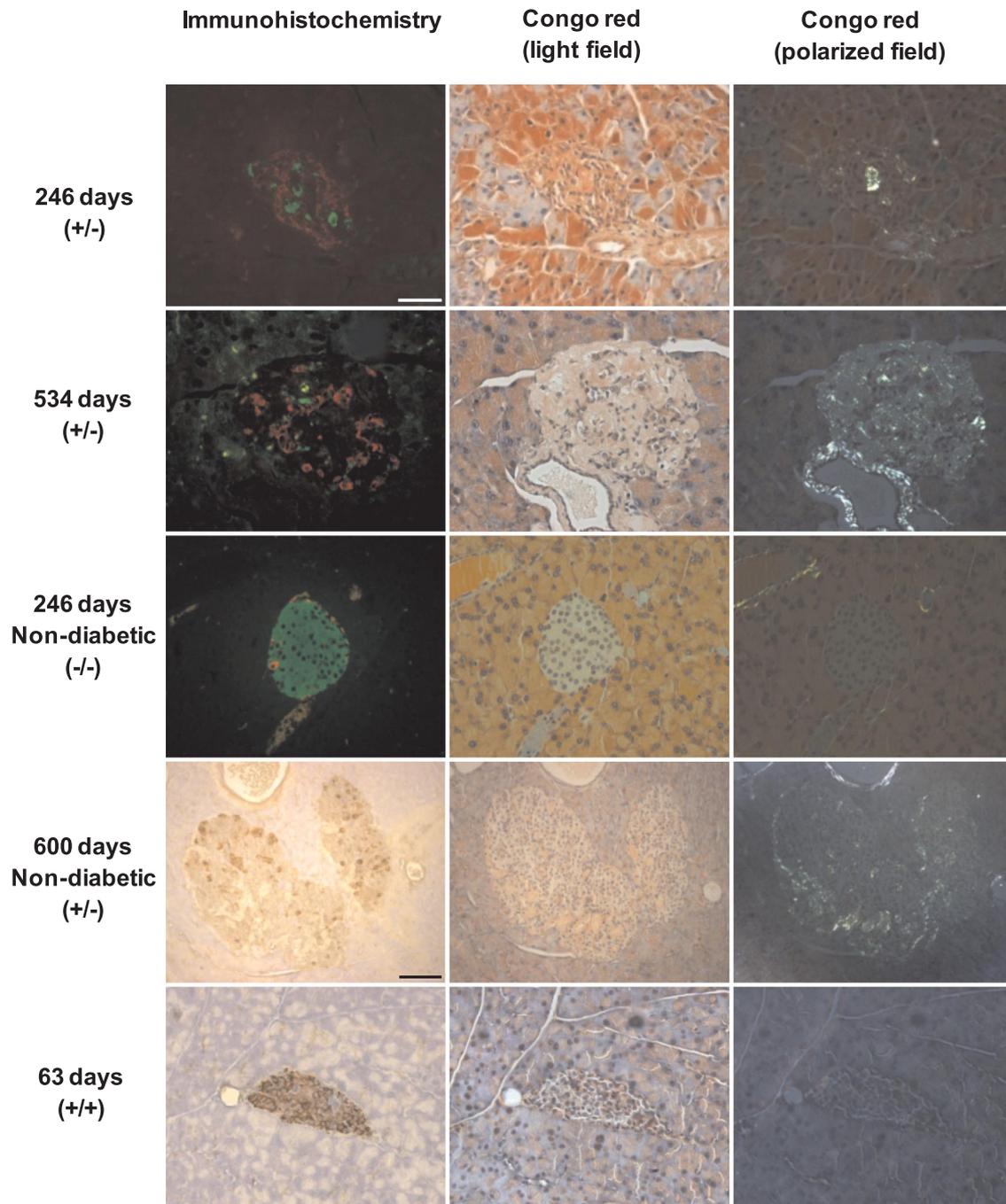
	Immunohistochemistry	Congo red (light field)	Congo red (polarized field)

FIG. 2. Amyloid visualized by light microscopy was dissociable from occurrence of diabetes in hemizygous hA/hIAPP transgenic mice. Photomicrographs show serial pancreatic islet sections from nontransgenic and human amylin transgenic animals. Left photomicrographs from *top three panels* show insulin (green) and glucagon (red) immunoreactivity. *Bottom two left photomicrographs* show islet sections incubated with antisera to somatostatin and glucagon revealing brown cytoplasmic staining. *Middle* and *right panels* show corresponding light- and polarized-microscopic field views of adjacent islet sections stained with Congo red. Amyloid birefringence is apple green, whereas that corresponding to collagen is silvery. The scale bar (50 μm) shown in *top left photomicrograph* applies to all images except for those corresponding to the 600-day nondiabetic hemizygous mouse (second to *bottom row*), which represents 100 μm. (A high-quality color digital representation of this figure is available in the online issue.)

cohorts of animals with or without equivalent tetracycline treatment (Fig. 4). Hemizygous mice were administered tetracycline in their drinking water from 30 days postweaning at 0.5 mg/ml to approximate the increased drug intake observed during polydipsia in the previous study. GTTs performed on a hemizygous cohort revealed no baseline differences (0 days treatment; Fig. 4A) but significantly improved glucose tolerance in the tetracycline-treated mice compared with water-treated controls at 30 days (Fig. 4B)

and 60 days treatment (Fig. 4C). Survival analysis indicated a trend toward delayed diabetes onset in the tetracycline-treated group ($P = 0.06$, data not shown).

In a parallel study, a second independent hemizygous cohort was treated with or without tetracycline immediately postweaning. ITTs performed after 60 and 90 days treatment showed that improved glucose tolerance was not due to any insulin-sensitizing effect of tetracycline (Fig. 4D and E). Tetracycline treatment also significantly delayed the median
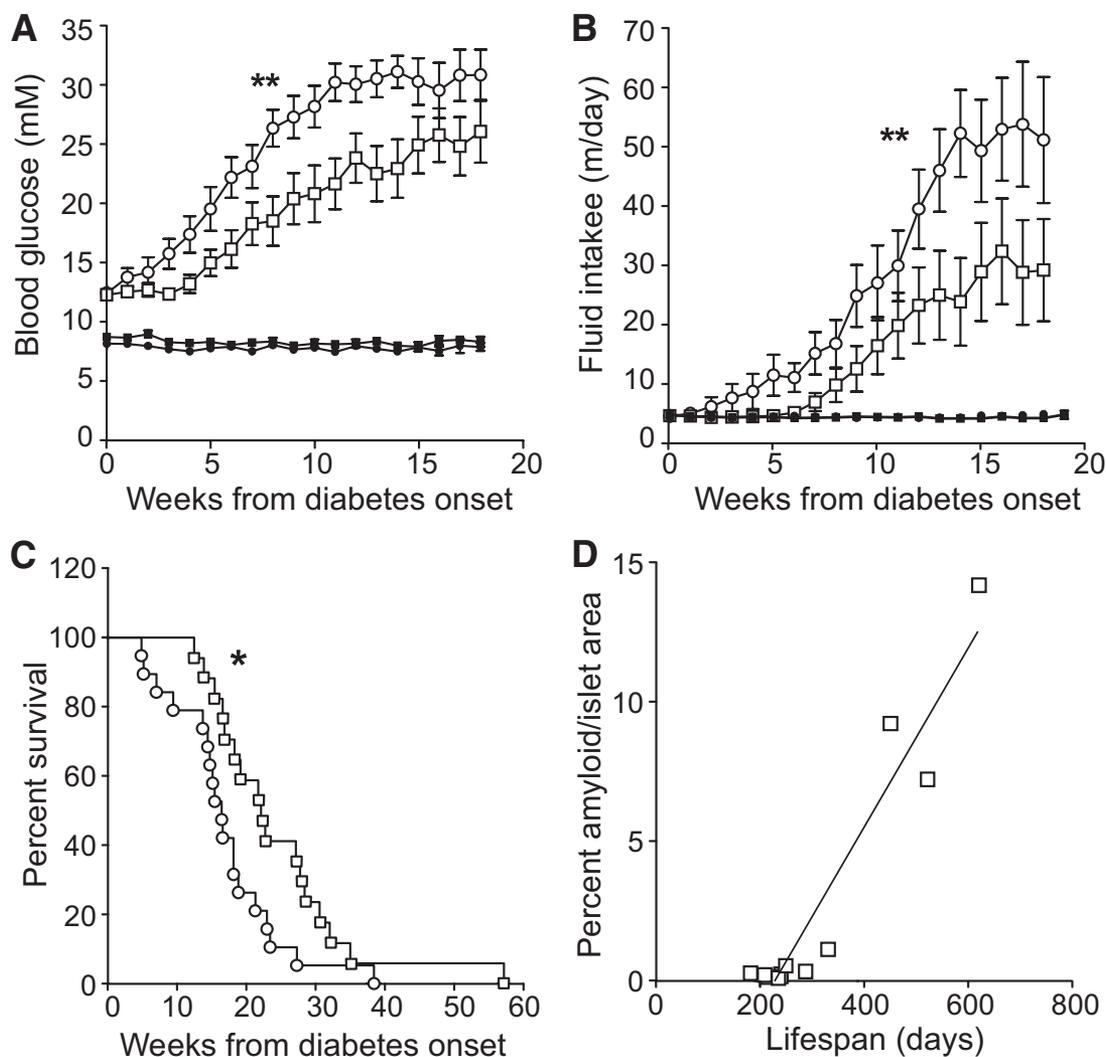
FIG. 3. Chronic administration of tetracycline (0.03 mg/ml of drinking water) in hemizygous mice from the time of weaning ameliorated diabetes and prolonged survival. Weekly blood glucose values (*A*) and fluid intake (*B*) in tetracycline-treated (□) versus water-treated (control) (○) animals. Each point represents the mean ± SE of values derived from $n = 7$–20 animals; (●, ■): values for corresponding nontransgenic littermates. Mean drug intake ($mg \cdot kg^{-1} \cdot day^{-1}$, mean ± SD) per animal was calculated from weekly fluid intake and weight measurements over the phases of pre-diabetes (5.4 ± 1, $n = 13$), diabetes to polydipsia (4.4 ± 0.7, $n = 16$), and polydipsia to death (44 ± 13, $n = 15$). Body weights at diabetes onset were also not significantly different between the control and drug-treated groups. Following onset of polydipsia, the tetracycline concentrations in the water of matched nontransgenic littermates were increased proportionately to maintain matched drug intake, and no adverse effects on fluid palatability were observed. Within the transgenic control group, 2 of 22 mice that spontaneously developed diabetes were omitted from the final analysis due to development of an eye infection and a tumor, respectively, whereas no animals were excluded from the tetracycline-treated transgenic group. *C*: Percent survival from diabetes onset (□, $n = 17$; ○, $n = 19$). **$P < 0.01$; *$P < 0.05$. *D*: Relationship between total area of amyloid deposits and lifespan in tetracycline-treated mice ($P < 0.001$, $n = 12$, $R^2 = 0.91$).

time to diabetes onset in this cohort of mice as compared with the corresponding water-treated control group (Fig. 4*F*, 98 vs. 66 days, $P < 0.05$). These studies showed that improved glucose tolerance and delayed onset of diabetes in tetracycline-treated hemizygous mice were not due to extrapancreatic insulin-sensitizing actions or other putative systemic effects of tetracycline on glucose homeostasis.

Amelioration of diabetes and increased lifespan by tetracycline were dosage dependent (study 3). To replicate and extend our previous findings, in particular with regard to dosage-related effects, further groups of hemizygous animals that had been administered water from the time of weaning were randomly assigned at the time of disease onset to one of the following groups: water-only control ($n = 12$), water containing 0.03 mg/ml tetracycline ($n = 12$) (study 3a, Fig. 5), or water containing 0.5 mg/ml tetracycline ($n = 10$) (study 3b, Fig. 5). The extent of suppression of disease progression in the tetra-

cycline-treated groups was dosage dependent with significant alleviation of hyperglycemia ($P < 0.01$; Fig. 5*A*) and corresponding fluid intake ($P < 0.05$; Fig. 5*B*) in the 0.5 mg/ml tetracycline–treated group compared with the water-treated controls. The 0.5 mg/ml tetracycline–treated group had a 254% increase in median survival from diabetes onset to death compared with the water-treated control group (208 vs. 82 days, respectively, $P < 0.05$; Fig. 5*C*), and there was a significant trend to dosage dependency among the three groups ($P < 0.05$).

Diabetes pathogenesis in hemizygous mice occurred through islet β-cell dysfunction followed by β-cell loss. To examine more precisely the effects of tetracycline treatment on islet β-cell mass, pancreatic islets were examined in a further independent cohort of diabetic mice studied at 6 weeks after disease onset. Hemizygous animals were randomly assigned at disease onset to one of two groups: either water-treated control or treatment with
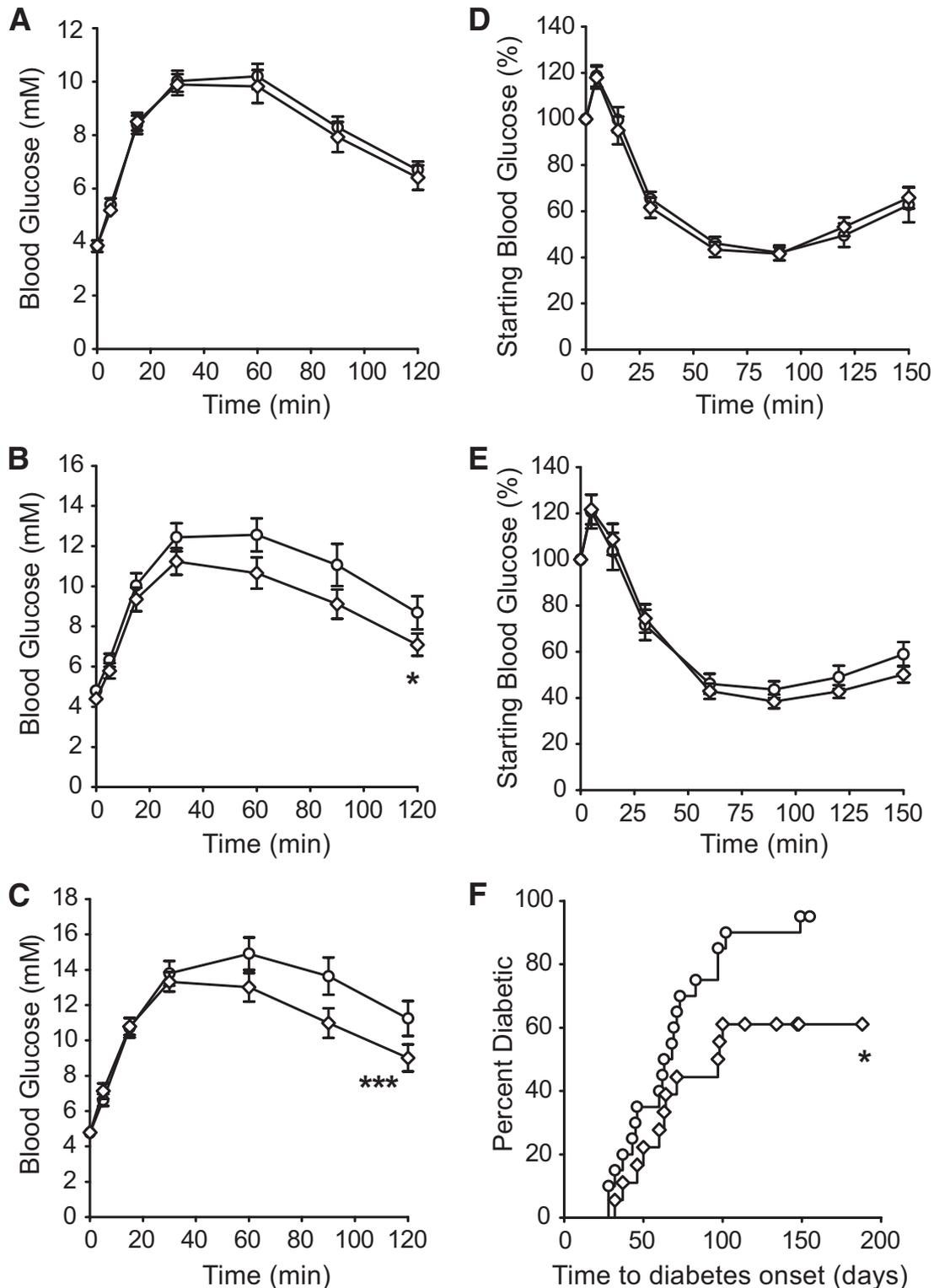
FIG. 4. Tetracycline (0.5 mg/ml of drinking water) improved glucose tolerance and delayed diabetes onset. Glucose tolerance tests were compared between tetracycline-treated ($\Diamond$) and control water-treated ($\bigcirc$) hemizygous mice at baseline (time = 0) (*A*) and after 30 (*B*) and 60 (*C*) days treatment. Statistical analysis by two-way ANOVA showed that curves corresponding to tetracycline-treated and control animals differed significantly after both 30 ($P < 0.01$) and 60 ($P < 0.001$) days treatment. Insulin tolerance tests were carried out in a second cohort of animals after 60 (*D*) and 90 (*E*) days equivalent tetracycline treatment. Each point represents the means ± SE of values derived from n = 12–25 animals. *F*: Survival analysis for the second cohort showed significantly delayed diabetes onset in tetracycline-treated mice (n = 18) versus the water-treated control group (n = 20). ***$P < 0.01$; *$P < 0.05$. In other experiments with nontransgenic littermates, glucose tolerance and insulin tolerance tests performed at 0, 60, and 90 days treatment showed that tetracycline administration did not intrinsically affect glucose tolerance or insulin sensitivity (not shown).
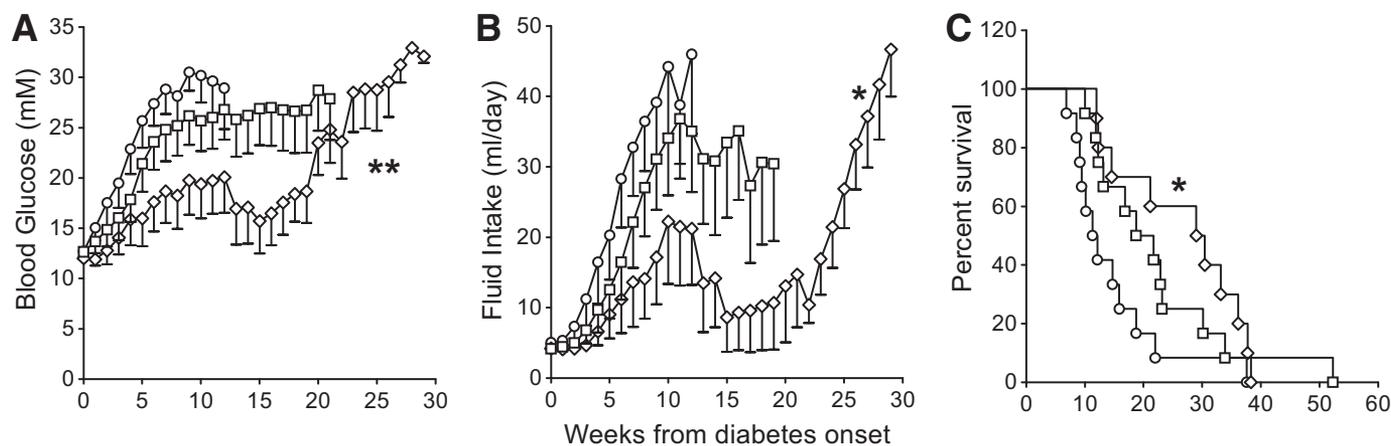
FIG. 5. Suppression of diabetes progression by tetracycline treatment was dosage dependent. Tetracycline was administered to hemizygous animals from the time of diabetes onset at concentrations of either 0.03 mg/ml (□) or 0.5 mg/ml (◇) of drinking water and results compared with those in water-treated control animals (○). Weekly blood glucose values (A) and fluid intakes (B) are shown. Data are means ± SE of values derived from 6 to 12 animals per point. **P < 0.01; *P < 0.05 for the 0.5 mg/ml tetracycline-treated compared with water-treated control hemizygous animals. C: Percent survival shown is in animals treated with 0.03 mg/ml tetracycline (n = 12, P = 0.08) or 0.5 mg/ml tetracycline (n = 10, P < 0.05) compared with those receiving water only (n = 12). There was no significant difference in bodyweight at diabetes onset or in the median time to diabetes onset across all three diabetic groups, nor did tetracycline exert effects on bodyweight as indicated by similar growth rates of tetracycline-treated and nontransgenic littermates. No animals were excluded from these analyses.

0.5 mg/ml tetracycline, as was described above for study 3b. Interestingly, visual inspection of islets from hemizygous mice with early- to mid-stage diabetes (Fig. 6A) showed they were structurally well preserved, with insulin areas similar to those of matched nontransgenic littermates (Fig. 6B). Also, quantitative analyses of islet areas revealed no significant between-group difference at this time-point (Fig. 6C). By contrast, animals with advanced diabetes had comparatively elevated blood glucose concentrations and reduced insulin areas, consistent with islet β-cell loss (Fig. 6D).

These qualitative observations were confirmed in an exhaustive, quantitative blinded comparison of insulin areas of 9–30 islets from individual tetracycline-treated (Fig. 6E) and water-treated (Fig. 6F) hemizygous mice. Although there was no significant difference in mean insulin area–to–islet area ratios between the two groups (75 ± 4%, n = 8 vs. 71 ± 7%, n = 12, respectively), there was a significant difference in their variance (F test, P = 0.029), pointing to a between-group difference. This finding was extended in further correlational analyses, which showed that there were significant inverse relationships between blood glucose concentrations and mean islet insulin area in each group (Fig. 6G). Here, there was a significant difference in the regression slopes between tetracycline- and water-treated mice (Fig. 6G). In particular, insulin area–to–islet area ratios in diabetic hemizygous mice, wherein blood glucose concentrations were <15 mmol/l, were comparable not only between tetracycline and water-treated mice but also with values in nontransgenic nondiabetic mice, for example as represented by mouse no. 352 (Fig. 6G, ◆).

We quantified pancreatic and serum insulin concentrations by ELISA in further separate groups of hemizygous mice 6 weeks after the onset of diabetes. Interestingly, although some reduction in total pancreatic insulin content was evident in some animals, there was no apparent relationship between insulin content and blood glucose concentrations (Fig. 6H). Similarly, there was no evident reduction in serum insulin concentrations, and indeed some hemizygous animals displayed comparatively high serum insulin concentrations during early diabetes (Fig.

6I). These findings showed that insulin area was maintained within the islets during early- and mid-stage diabetes in hemizygous transgenic mice with no substantial reductions in pancreatic insulin content or serum insulin concentrations. They are consistent with islet β-cell loss as a correlate of later-stage, more severe diabetes (blood glucose >15 mmol/l).

DISCUSSION

Our findings demonstrate that the amyloid deposits found in the pancreatic islets of hA/hIAPP transgenic mice are not intrinsically cytotoxic, an observation consistent with the reported occurrence of islet amyloid in nondiabetic humans (2). Perhaps most notably, amyloid deposition was not observed in homozygous animals with severe, early-onset diabetes but was present in both diabetic and nondiabetic hemizygous animals, where it was positively rather than negatively correlated with lifespan.

In homozygous transgenic animals, the lack of visible amyloid deposition coupled with the higher intrinsic hA/hIAPP expression and significantly depleted pancreatic insulin concentrations at the median time to diabetes onset were all consistent with islet β-cell loss as the major diabetogenic mechanism. Evidence from other hA/hIAPP transgenic murine lines has pointed to a role for soluble oligomers in the increased frequency of β-cell apoptosis in late-stage diabetes (15,18,19). The corresponding lack of amyloid in our homozygous mice is consistent with this pathogenic mechanism and supports a growing body of experimental data consistent with the hypothesis that cytotoxic effects of prefibrillar aggregates of other amyloidogenic proteins, such as β-amyloid and α-synuclein, can elicit cell death (33–37).

Our findings also show that tetracycline can partially suppress the progression of diabetes in hemizygous animals. In study 1, it slowed the rate of deterioration in blood glucose and polydipsia after diabetes onset, compared with matched control animals, which translated into a 34% increase in median survival. By contrast, tetracycline did not delay diabetes onset in this study, although the lack of an effect may simply have reflected the
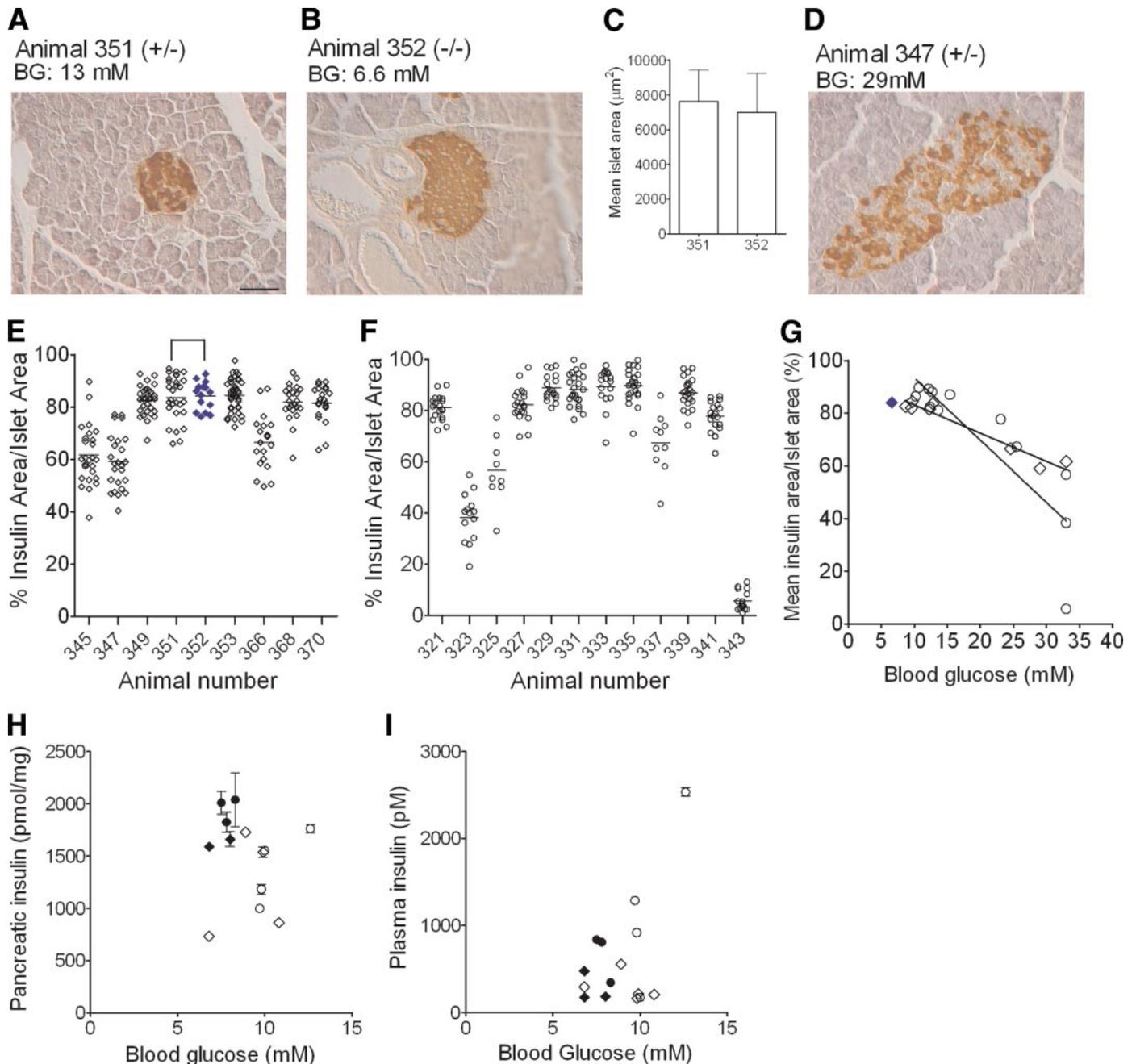
FIG. 6. Quantitative islet immunohistochemistry indicates that β-cell dysfunction preceded β-cell loss in diabetic hemizygous mice. Pancreatic islets were analyzed by blinded insulin histochemistry in hemizygous and matched nondiabetic control mice at time points that corresponded to 6 weeks after diabetes onset in each transgenic mouse. *A*: Insulin staining in a representative islet from a tetracycline-treated (0.5 mg/ml) transgenic mouse (animal no. 351, +/−). *B*: An islet from its corresponding matched nontransgenic control (animal no. 352, −/−). *C*: Islet areas did not differ significantly between these two animals. By contrast, shown in *D*, is an islet from a hemizygous animal with markedly elevated blood glucose accompanied by a decreased area of islet insulin staining. Scale bar represents 50 μm. Quantitative analyses of insulin area–to–islet area ratios from 9 to 30 islets per animal are shown in a series of individual tetracycline-treated ($n = 9$) (*E*) or water-treated ($n = 12$) (*F*) diabetic hemizygous transgenic mice; each datum point represents the ratio from a single islet and horizontal lines are arithmetic means. For comparison, islet analyses for animal no. 352, which is the tetracycline-treated nontransgenic and nondiabetic age-matched control for hemizygous animal no. 351, are shown in *E* as closed blue diamonds. *G*: Linear correlation analysis of the relationships between blood glucose values and insulin area–to–islet area ratios were demonstrated in both groups (both $P < 0.0001$); there was also a significant difference between the slopes of the curves in the two groups ($P < 0.0001$); the solid blue diamond corresponds to the nontransgenic animal whose islet was shown in *B*. Blood glucose and pancreatic insulin content (*H*) and serum insulin concentrations (*I*) in animals ($n = 3$ replicates/mouse); these latter analyses were performed in separate cohorts of water-treated (○) and tetracycline-treated (0.5 mg/ml, ◇) hemizygous mice studied at the time point 6 weeks after diabetes onset. Data from matched nontransgenic and nondiabetic mice studied at the corresponding time point are indicated by closed black symbols. Data in *C*, *H*, and *I* are means ± SE. *A*, *B*, and *D*: BG, blood glucose. (A high-quality color digital representation of this figure is available in the online issue.)

relatively low dosage administered during the pre-diabetic phase. The likelihood that this explanation is correct was confirmed in study 2, wherein tetracycline administration at the higher dosage of 0.5 mg/ml from 30 days after

weaning, significantly delayed disease onset and progression. The observed improvement in glucose tolerance in tetracycline-treated hemizygous mice after 30 and 60 days of treatment is also consistent with observations from

study 3, where we again used the higher drug dosage (0.5 mg/ml) but with administration from the time of disease onset. In this study, tetracycline exerted a clear, dosage-dependent effect to delay the deterioration in blood glucose regulation and polydipsia, with the higher dosage causing an increase in median survival of 254% in the period following diabetes onset.

We found no evidence that the antidiabetes effects evoked by tetracycline in the hemizygous mice were due to any putative extrapancreatic effects, since ITTs revealed that it exerted no detectable systemic insulin-sensitizing effects in either hemizygous mice or their nontransgenic littermates. Furthermore, tetracycline had no measurable effects on glucose regulation in nontransgenic littermates. When taken together with the histological analysis of islets 6 weeks after diabetes onset, these data point toward preservation of islet β-cell function as the mechanism underlying tetracycline's actions to delay onset and progression of diabetes, possibly through interactions with soluble nascent prefibrillar aggregates.

Finally, our findings show that β-cell dysfunction and not β-cell loss was responsible for the initial development of diabetes in these hemizygous mice. Compared with the rapid onset and development of diabetes in homozygous animals, diabetes onset and progression were significantly more gradual in the hemizygous group. Strikingly, nontransgenic controls and hemizygous animals had similar total pancreatic insulin content at the median time of diabetes onset. Significantly, their insulin areas were also comparable in the early- and mid-stages of diabetes, indicating that no significant loss of β-cells had ensued to this point in disease progression. Direct measurements of pancreatic and serum insulin concentrations 6 weeks following diabetes onset, although variable, were also consistent with the above finding, in that there were no substantive reductions in insulin content and no clear associations with blood glucose concentrations. This effect is consistent with the development of glucose blindness in the islets of at least some hemizygous mice (38).

Our experimental analyses were clearly able to discriminate a 20% loss in insulin staining area or in islet β-cell mass, but such absolute reductions only occurred in association with advanced diabetes. That no significant reduction in insulin staining area occurred in early- to mid-stage diabetes clearly demonstrates that hA/hIAPP expression does not initially evoke diabetes in hemizygous mice by eliciting overt islet β-cell loss. In support of this conclusion, extensive immunohistochemical analyses revealed no evidence for β-cell apoptosis in pancreatic sections from hemizygous mice 6 weeks following diabetes onset, as measured by caspase-3 or terminal deoxynucleotidyl transferase-mediated dUTP nick-end labeling staining (data not shown), although the assays we used may have been insufficiently sensitive to detect rare apoptotic cells in affected islets.

Our findings indicate that below a certain threshold, hA/hIAPP expression causes islet β-cell dysfunction leading to impaired insulin production, processing, and/or secretion at the outset of diabetes (14). Here, we could not investigate insulin processing due to the unavailability of an appropriate mouse-specific proinsulin ELISA. As amylin expression in our mice is under control of the rat insulin 2 promoter, we expect that rising blood glucose would establish a positive feedback cycle that progressively facilitates islet β-cell loss. Presumably, this latter mechanism occurs by default in homozygous mice which possess higher intrinsic hA/hIAPP expression.

In summary, our findings show that islet β-cell dysfunction and not mature extracellular amyloid is the underpinning cause for diabetes pathogenesis in hemizygous hA/hIAPP transgenic mice. Moreover, deposition of microscopically visible amyloid was positively correlated with lifespan, showing that tissue hA/hIAPP deposits are not intrinsically cytotoxic. Treatment with an effective dosage of tetracycline delayed the onset and impeded the progression of diabetes in hemizygous mice. Consequently, any intervention that allows progressive deposition of (apparently benign) islet amyloid through mechanisms that reduce the cytotoxicity of prefibrillar aggregates might be expected to prevent islet β-cell degeneration.

REFERENCES

1. Butler AE, Janson J, Bonner-Weir S, Ritzel R, Rizza RA, Butler PC. β-Cell deficit and increased β-cell apoptosis in humans with type 2 diabetes. Diabetes 2003;52:102–110
2. Zhao HL, Lai FM, Tong PC, Zhong DR, Yang D, Tomlinson B, Chan JC. Prevalence and clinicopathological characteristics of islet amyloid in Chinese patients with type 2 diabetes. Diabetes 2003;52:2759–2766
3. Opie EL. The relation of diabetes mellitus to lesions of the pancreas: hyaline degeneration of the islands of Langerhans. J Exp Med 1901;5:527–540
4. Cooper GJS, Willis AC, Clark A, Turner RC, Sim RB, Reid KBM. Purification and characterization of a peptide from amyloid-rich pancreases of type 2 diabetic patients. Proc Natl Acad Sci U S A 1987;84:8628–8632
5. Westermark P, Wernstedt C, Wilander E, Hayden DW, O'Brien TD, Johnson KH. Amyloid fibrils in human insulinoma and islets of Langerhans of the diabetic cat are derived from a neuropeptide-like protein also present in normal islet cells. Proc Natl Acad Sci U S A 1987;84:3881–3885
6. Goldsbury C, Goldie K, Pellaud J, Seelig J, Frey P, Muller SA, Kistler J, Cooper GJ, Aebi U. Amyloid fibril formation from full-length and fragments of amylin. J Struct Biol 2000;130:352–362
7. Konarkowska B, Aitken JF, Kistler J, Zhang S, Cooper GJ. The aggregation potential of human amylin determines its cytotoxicity towards islet beta-cells. FEBS J 2006;273:3614–3624
8. Janciauskiene S, Ahren B. Different sensitivity to the cytotoxic action of IAPP fibrils in two insulin-producing cell lines, HIT-T15 and RINm5F cells. Biochem Biophys Res Commun 1998;251:888–893
9. Zhang S, Liu J, Saafi EL, Cooper GJ. Induction of apoptosis by human amylin in RINm5F islet β-cells is associated with enhanced expression of p53 and p21WAF1/CIP1. FEBS Lett 1999;455:315–320
10. Zhang S, Liu H, Yu H, Cooper GJ. Fas-associated death receptor signaling evoked by human amylin in islet β-cells. Diabetes 2008;57:348–356
11. Zhang S, Liu J, MacGibbon G, Dragunow M, Cooper GJ. Increased expression and activation of c-Jun contributes to human amylin-induced apoptosis in pancreatic islet β-cells. J Mol Biol 2002;324:271–285
12. Zhang S, Liu H, Liu J, Tse CA, Dragunow M, Cooper GJ. Activation of activating transcription factor 2 by p38 MAP kinase during apoptosis induced by human amylin in cultured pancreatic beta-cells. FEBS J 2006;273:3779–3791

13. Zhang S, Liu J, Dragunow M, Cooper GJ. Fibrillogenic amylin evokes islet β-cell apoptosis through linked activation of a caspase cascade and JNK1. J Biol Chem 2003;278:52810–52819

14. Haataja L, Gurlo T, Huang CJ, Butler PC. Islet amyloid in type 2 diabetes, and the toxic oligomer hypothesis. Endocr Rev 2008;29:303–316

15. Janson J, Soeller WC, Roche PC, Nelson RT, Torchia AJ, Kreutter DK, Butler PC. Spontaneous diabetes mellitus in transgenic mice expressing human islet amyloid polypeptide. Proc Natl Acad Sci U S A 1996;93:7283–7288

16. Soeller WC, Janson J, Hart SE, Parker JC, Carty MD, Stevenson RW, Kreutter DK, Butler PC. Islet amyloid-associated diabetes in obese A(vy)/a mice expressing human islet amyloid polypeptide. Diabetes 1998;47:743–750

17. Höppener JW, Oosterwijk C, Nieuwenhuis MG, Posthuma G, Thijssen JH, Vroom TM, Ahren B, Lips CJ. Extensive islet amyloid formation is induced by development of type II diabetes mellitus and contributes to its progression: pathogenesis of diabetes in a mouse model. Diabetologia 1999;42:427–434

18. Butler AE, Janson J, Soeller WC, Butler PC. Increased β-cell apoptosis prevents adaptive increase in β-cell mass in mouse model of type 2 diabetes: evidence for role of islet amyloid formation rather than direct action of amyloid. Diabetes 2003;52:2304–2314

19. Butler AE, Jang J, Gurlo T, Carty MD, Soeller WC, Butler PC. Diabetes due to a progressive defect in β-cell mass in rats transgenic for human islet amyloid polypeptide (HIP Rat): a new model for type 2 diabetes. Diabetes 2004;53:1509–1516

20. Scrocchi LA, Chen Y, Waschuk S, Wang F, Cheung S, Darabie AA, McLaurin J, Fraser PE. Design of peptide-based inhibitors of human islet amyloid polypeptide fibrillogenesis. J Mol Biol 2002;318:697–706

21. Forloni G, Colombo L, Girola L, Tagliavini F, Salmona M. Anti-amyloidogenic activity of tetracyclines: studies in vitro. FEBS Lett 2001;487:404–407

22. Cardoso I, Merlini G, Saraiva MJ. 4′-iodo-4′-deoxydoxorubicin and tetracyclines disrupt transthyretin amyloid fibrils in vitro producing noncytotoxic species: screening for TTR fibril disrupters. FASEB J 2003;17:803–809

23. Tagliavini F, Forloni G, Colombo L, Rossi G, Girola L, Canciani B, Angeretti N, Giampaolo L, Peressini E, Awan T, De Gioia L, Ragg E, Bugiani O, Salmona M. Tetracycline affects abnormal properties of synthetic PrP peptides and PrP(Sc) in vitro. J Mol Biol 2000;300:1309–1322

24. Hogan BL, Costantini F, Lacy E: *Manipulating the Mouse Embryo: A Laboratory Manual.* Cold Spring Harbor, NY, Cold Spring Harbor Laboratory Press, 1986

25. Sambrook J, Fritsch EF, Maniatis T: *Molecular Cloning: A Laboratory Manual.* 2nd ed. Cold Spring Harbor, NY, Cold Spring Harbour Laboratory, 1989

26. Church GM, Gilbert W. Genomic sequencing. Proc Natl Acad Sci U S A 1984;81:1991–1995

27. van Hulst KL, Born W, Muff R, Oosterwijk C, Blankenstein MA, Lips CJ, Fischer JA, Höppener JW. Biologically active human islet amyloid polypeptide/amylin in transgenic mice. Eur J Endocrinol 1997;136:107–113

28. Kahn SE, Andrikopoulos S, Verchere CB, Wang F, Hull RL, Vidal J. Oophorectomy promotes islet amyloid formation in a transgenic mouse model of type II diabetes. Diabetologia 2000;43:1309–1312

29. Geisler JG, Zawalich W, Zawalich K, Lakey JR, Stukenbrok H, Milici AJ, Soeller WC. Estrogen can prevent or reverse obesity and diabetes in mice expressing human islet amyloid polypeptide. Diabetes 2002;51:2158–2169

30. Platt N, da Silva RP, Gordon S. Recognizing death: the phagocytosis of apoptotic cells. Trends Cell Biol 1998;8:365–372

31. Aitken JF, Loomes KM, Konarkowska B, Cooper GJ. Suppression by polycyclic compounds of the conversion of human amylin into insoluble amyloid. Biochem J 2003;374:779–784

32. Smith DL, Woodman B, Mahal A, Sathasivam K, Ghazi-Noori S, Lowden PA, Bates GP, Hockly E. Minocycline and doxycycline are not beneficial in a model of Huntington's disease. Ann Neurol 2003;54:186–196

33. Janson J, Ashley RH, Harrison D, McIntyre S, Butler PC. The mechanism of islet amyloid polypeptide toxicity is membrane disruption by intermediate-sized toxic amyloid particles. Diabetes 1999;48:491–498

34. Hardy J, Selkoe DJ. The amyloid hypothesis of Alzheimer's disease: progress and problems on the road to therapeutics. Science 2002;297:353–356

35. Lambert MP, Barlow AK, Chromy BA, Edwards C, Freed R, Liosatos M, Morgan TE, Rozovsky I, Trommer B, Viola KL, Wals P, Zhang C, Finch CE, Krafft GA, Klein WL. Diffusible, nonfibrillar ligands derived from Aβ1–42 are potent central nervous system neurotoxins. Proc Natl Acad Sci U S A 1998;95:6448–6453

36. Goldberg MS, Lansbury PT Jr: Is there a cause-and-effect relationship between alpha-synuclein fibrillization and Parkinson's disease? Nat Cell Biol 2000;2:E115–119

37. Sousa MM, Cardoso I, Fernandes R, Guimaraes A, Saraiva MJ. Deposition of transthyretin in early stages of familial amyloidotic polyneuropathy: evidence for toxicity of nonfibrillar aggregates. Am J Pathol 2001;159:1993–2000

38. Andrikopoulos S, Verchere CB, Terauchi Y, Kadowaki T, Kahn SE. β-Cell glucokinase deficiency and hyperglycemia are associated with reduced islet amyloid deposition in a mouse model of type 2 diabetes. Diabetes 2000;49:2056–2062

39. Percy AJ, Trainor DA, Rittenhouse J, Phelps J, Koda JE. Development of sensitive immunoassays to detect amylin and amylin-like peptides in unextracted plasma. Clin Chem 1996;42:576–585